Cocrystallization and Phase Segregation of Polyethylene Blends. 2. Synchrotron-Sourced X-ray Scattering and Small-Angle Light Scattering Study of the Blends between the D and H Species

Kohji Tashiro,*,†,‡ Michael M. Satkowski,§ Richard S. Stein,‡ Yingjie Li,∥ Benjamin Chu,∥ and Shaw L. Hsu‡

Department of Polymer Science and Engineering, University of Massachusetts, Amherst, Massachusetts 01003, Miami Valley Laboratories, Procter & Gamble Company, Ltd., P.O. Box 398707, Cincinnati, Ohio 45239-8707, and Department of Chemistry, State University of New York at Stony Brook, Long Island, New York 11794-3400

Received May 15, 1991; Revised Manuscript Received December 7, 1991

ABSTRACT: The cocrystallization and phase segregation phenomena reported in the preceding paper of this issue have been reconfirmed by measuring the temperature dependence of the wide-angle (WAXS) and small-angle X-ray scatterings (SAXS) using synchrotron radiation for the blend systems of deuterated high-density polyethylene with hydrogenous polyethylene species having various branching contents. On the basis of the WAXS, SAXS, and small-angle light scattering data in addition to the Fourier transform infrared spectral data reported previously, a difference in the crystal structure, lamellar structure, and spherulite structure has been compared between the blend samples with various degrees of branching.

Introduction

Blends of high-density and (linear) low-density polyethylene (PE) samples have attracted much attention because of their practical usages and basic scientific interests.[1-12] It may be very important to clarify roles of each component involved in the crystallization behavior of the blends. Unfortunately, however, high-density PE (HDPE) and linear low-density PE (LLDPE) or low-density PE (LDPE) have the same chemical species of C and H, and so it is quite difficult to distinguish their behaviors separately by using the conventional physicochemical methods. In the preceding paper,[13] we utilized a fully deuterated high-density PE (DHDPE) sample as one component and investigated the crystallization behaviors of PE blends between DHDPE and the hydrogenous samples with various branching contents. In that study,[13] FTIR spectral measurements were found to be quite useful to clarify the behaviors of the D and H components in the blends separately at the molecular level. Among the various types of PE blends with DHDPE, the blend of a linear low-density (LLDPE) sample having a relatively low branching content was found to exhibit an almost perfect cocrystallization phenomenon of the CH_2 and CD_2 species within the same crystallite. The degree of such a cocrystallization depends on the branching content of the hydrogenous sample. For example, in Figure 1 is reproduced the correlation of the coefficient k_c of the CH_2 and CD_2 species in the DHDPE blends with HDPE, LLDPE(2), and LLDPE(3); the characterization results of these samples are listed in Table I.[13] The k_c in Figure 1 is defined as a coefficient with which the infrared spectrum B of the blend is approximately expressed as a simple summation of the spectra of crystalline (C) and amorphous (A) phases: $B = k_cC + (1 - k_c)A$. The k_c can be used as a measure of the crystalline content. In the case of LLDPE(2) a good correlation is observed between H and D species; the crystallization bands of the H and D species begin to appear simultaneously at the same temperature and increase their intensity with cooling temperature. For the blend with HDPE the CH_2 species crystallize at first and then the other species CD_2 begin to crystallize in the lower temperature region, indicating a phase segregation. For the blend with LLDPE(3), the situation is the same as the case with HDPE but the order of CD_2 and CH_2 should be exchanged. Generally speaking, however, the FTIR spectra in the so-called fingerprint region reflect a localized structural feature of the crystalline (and amorphous) phase. The X-ray diffraction method is useful to investigate the averaged behavior of the whole crystallites; in particular, a combination of wide-angle (WAXS) and small-angle X-ray scatterings (SAXS) may be very powerful for establishing the cocrystallization and

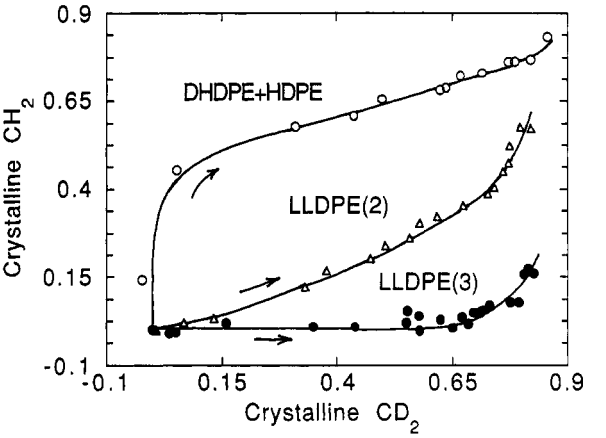

Figure 1. Correlation of the crystalline coefficient k_c between the CH_2 and CD_2 crystalline bands for a series of the DHDPE blend samples with (a) HDPE, (b) LLDPE(2), and (c) LLDPE(3).

Table I
Characterization of PE Samples

	M_w	M_n	M_w/M_n	branching[a]
DHDPE	80K	14K	5.7	2–3
LLDPE(2)	75K	37K	2.0	17
LLDPE(3)	61K	20K	3.1	41

[a] No. of short chains/1000 carbons.

† Permanent address: Department of Macromolecular Science, Faculty of Science, Osaka University, Toyonaka, Osaka 560, Japan.
‡ University of Massachusetts.
§ Procter & Gamble Co., Ltd.
∥ State University of New York at Stony Brook.

0024-9297/92/2225-1809$03.00/0

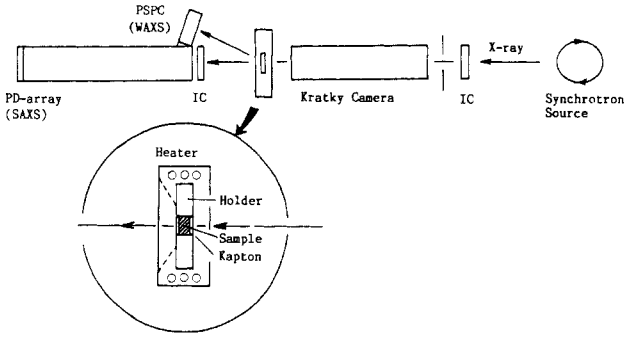

Figure 2. Illustration of the simultaneous measuring system of WAXS and SAXS using the synchrotron X-ray source. IC: ion chamber. PD: photodiode.

phase separation phenomena of the PE blends revealed by the infrared and DSC measurements. Furthermore, by combining the small-angle light scattering data with the data obtained by the above-mentioned various methods, we will be able to have a broader view of the structure of the blend system from the molecular level to the unit cell level, the lamellar level, and the spherulite level.

In the first half of this paper we will describe the experimental results on the temperature dependence of the WAXS and SAXS data for the two kinds of PE blends reported in the preceding paper,[13] i.e., DHDPE + LLDPE-(2) and DHDPE + LLDPE(3), and will confirm the phenomena of cocrystallization and phase segregation reported in that paper through the infrared spectral measurements. In the second half of this paper we will investigate the structure of these two blend systems at room temperature and discuss the crystallization mechanism based on the different levels of dimension from angstrom to micrometer.

Experimental Section

Samples. The PE samples are those just used in the DSC and FTIR measurements; DHDPE, LLDPE(2), and LLDPE(3). Their characterization was already listed in Table I.[13] The samples for the WAXS and SAXS experiments were prepared by inserting them into a round hole of the metal holder shown in Figure 2 and cooling from the melt to room temperature. The diameter of the samples is ca. 7 mm, and the thickness is ca. 1 mm.

Measurements. WAXS and SAXS patterns were measured at the National Synchrotron Light Source, Brookhaven National Laboratory, Long Island, NY. A thermocouple was in contact with the steel sample holder which was placed in the temperature-controlled chamber of the modified Kratky SAXS diffractometer. A rough illustration of the SAXS instrumentation is shown in Figure 2, where a Braun position-sensitive proportional counter was used as the detector for WAXS and a photodiode array detector was used for SAXS. The sample was melted and cooled to room temperature at about 1 °C/min, during which time both WAXS and SAXS data were collected simultaneously over every 2-min time period between 150 and 50 °C. The scattering profiles were corrected for detector nonuniformity, sample absorption, background, and incident X-ray intensity fluctuations.[11,12] In order to estimate the crystallite size and unit cell parameters at room temperature more exactly, WAXS patterns were also collected using a conventional X-ray diffractometer.

The small-angle light scattering patterns of the blends were taken by using either a film or an optical multichannel detector with a laser light source of 632.8-nm wavelength under the polarization condition of H_V at room temperature.

Results and Discussion

Temperature Dependence of WAXS and SAXS. (A) Blend System of DHDPE + LLDPE(2). As an example, Figure 3 shows the temperature dependence of

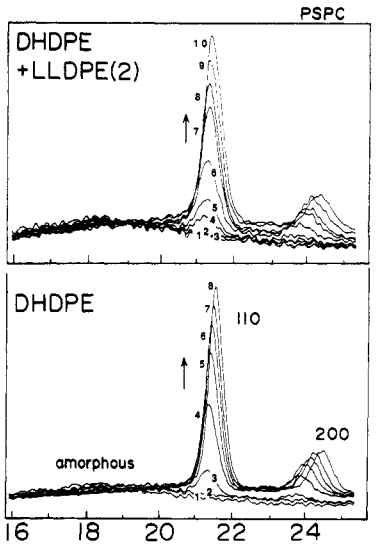

Figure 3. Temperature dependence of the WAXS pattern measured for (upper) the DHDPE + LLDPE(2) blend and (lower) the DHDPE pure sample in the cooling process from the melt. Temperatures are as follows. Upper: (1) 130, (2) 120, (3) 110, (4) 109, (5) 107, (6) 102, (7) 96, (8) 88, (9) 78, (10) 58 °C. Lower: (1) 130, (2) 120, (3) 114, (4) 110, (5) 100, (6) 88, (7) 78, (8) 60 °C.

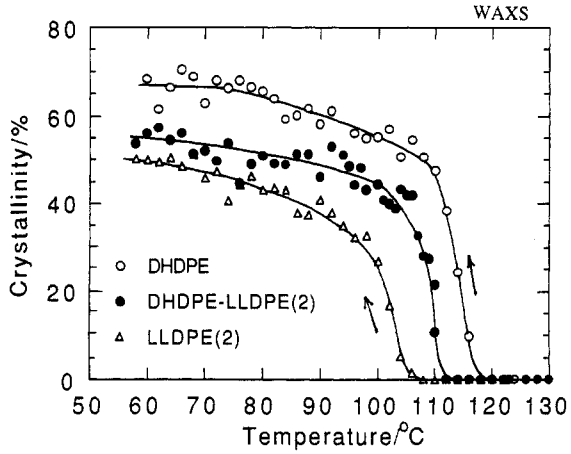

Figure 4. Temperature dependence of the degree of crystallinity estimated for the DHDPE + LLDPE(2) system using WAXS data.

the WAXS pattern measured for the blend of DHDPE with LLDPE(2) in comparison with that of DHDPE pure polymer during the cooling process from the melt. In the case of the blend, the reflection peaks of 110 and 200, intrinsic of the blend, can be observed to grow in parallel with a decrease in the amorphous halo peak intensity. An appearance of the reflections intrinsic of the blend indicates definitely the formation of a unique crystalline phase where the DHDPE and LLDPE(2) chains coexist. In Figure 4 are shown the temperature dependences of the degree of crystallinity (x) estimated from the integrated intensity of the X-ray scatterings shown in Figure 3;

$$x = \int_{\text{crystal}} Iq^2\,dq / \int_{\text{whole region}} Iq^2\,dq$$

where I is an intensity and q is a scattering vector. The degree of crystallinity begins to increase at a temperature quite different from those of the original pure samples, in good agreement with the temperature measured by DSC and FTIR.[13] The degree of crystallinity of the blend is between those of the original values.

In Figures 5 and 6 are shown the SAXS pattern changes measured for DHDPE, LLDPE(2), and their blend sample

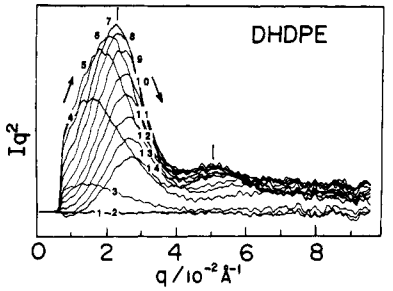

Figure 5. Temperature dependence of the SAXS pattern measured for the pure DHDPE sample (cooling process from the melt). Temperatures are as follows: (1) 124, (2) 119, (3) 117, (4) 114, (5) 112, (6) 110, (7) 104, (8) 100, (9) 96, (10) 92, (11) 87, (12) 79, (13) 72, (14) 61 °C.

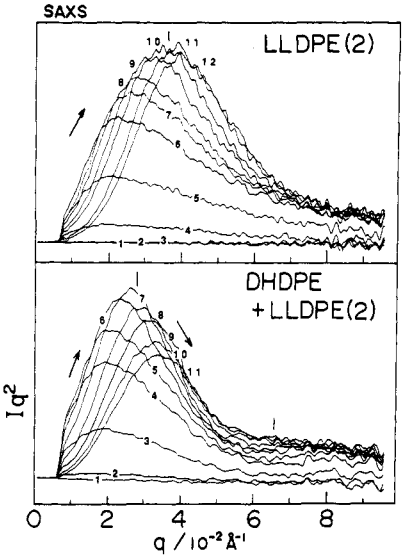

Figure 6. Temperature dependence of the SAXS pattern measured for the LLDPE(2) (upper) and DHDPE + LLDPE(2) (lower) systems (cooling process from the melt). Temperatures are as follows. Upper: (1) 119, (2) 112, (3) 106, (4) 102, (5) 100, (6) 98, (7) 96, (8) 94, (9) 88, (10) 75, (11) 65, (12) 60 °C. Lower: (1) 115, (2) 112, (3) 110, (4) 108, (5) 106, (6) 100, (7) 94, (8) 80, (9) 70, (10) 67, (11) 61 °C.

during slow cooling from the melts, where the background scattering is eliminated using the data of the melt state and the vertical axis is replotted using Iq^2 instead of the observed intensity I. In the case of the pure DHDPE sample, the SAXS pattern begins to increase in intensity at first and then decreases gradually. The second-order reflections can also be observed. In Figure 7 is plotted the integrated intensity or invariance Q against temperature; $Q = 4\pi\int Iq^2\,dq$. Q begins to increase rapidly at the initial stage of crystallization and then decreases gradually because the degree of crystallinity exceeds the value 50%. [According to the simple two-phase model of crystalline and amorphous regions, Q is proportional to $x(1-x)$.][14] As shown in Figure 6, the blend sample shows the SAXS pattern characteristic of itself and is different from the pattern expected for the simple overlap between the original two polymers. This indicates that the blend of DHDPE + LLDPE(2) can form an intrinsic aggregation structure of lamellae, different from those of the original ones. The rising-up temperature of the curve Q vs temperature is quite consistent with the WAXS data and locates between those of the pure polymers. The SAXS profile is sharp compared with that of the LLDPE(2) and shows even the second-order reflection just as likely as in the DHDPE case, suggesting a more regular repeating of lamellae over a longer range. Figure 8 shows the inter-

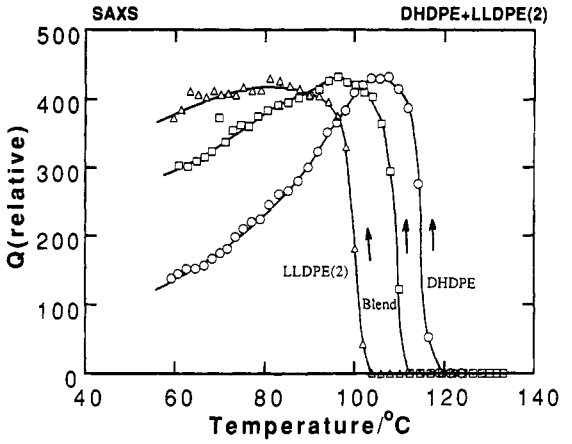

Figure 7. Temperature dependence of the invariance Q estimated from the SAXS data for the DHDPE + LLDPE(2) system.

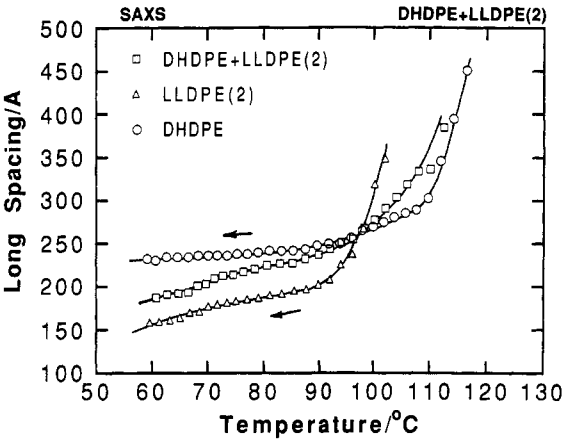

Figure 8. Temperature dependence of the long spacing estimated from the SAXS data for the DHDPE + LLDPE(2) system.

lamellar spacing evaluated from the peak position of the SAXS pattern for these samples. At the initial stage of crystallization the lamellar long spacing is very large because only a few lamellar nuclei are generated. As the crystallization proceeds the averaged lamellar distance decreases steeply and is stabilized gradually as the sample is cooled down to room temperature.[15] The long spacing of the blend system is shorter than that of the DHDPE but longer than that of the LLDPE(2).

In this way the WAXS and SAXS data allow us to establish the cocrystallization phenomenon in this blend system. The data also indicate that an aggregation structure of lamellae in the blend system is different from those of the pure components.

(B) Blend System of DHDPE + LLDPE(3). In Figure 9 are plotted the temperature dependences of the degree of crystallinity evaluated by WAXS for the DHDPE + LLDPE(3) system. Quite consistently with the DSC and FTIR data,[13] the blend sample shows the two-stage variation in the WAXS pattern or the degree of crystallinity; at first the crystalline reflections begin to appear around 115 °C, which is close to the crystallization temperature of the DHDPE component, and then change their behavior around 90 °C or the crystallization temperature of the LLDPE(3) sample. A small dip around 90 °C observed for the blend system is meaningful and comes from the change in the crystallization behavior between the DHDPE and LLDPE(3) components mentioned above.

The temperature changes in the SAXS pattern of the blend and of the pure LLDPE(3) sample were also measured. The blend sample exhibits rather sharp

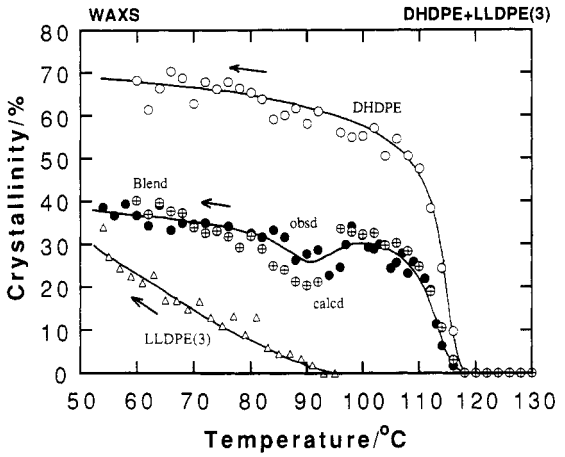

Figure 9. Temperature dependence of the degree of crystallinity estimated for the DHDPE + LLDPE(3) system using the WAXS data. In the curve of the blend, the filled circle is the observed data point and the crossed circle is the point calculated using the observed values of the pure DHDPE and LLDPE(3) samples.

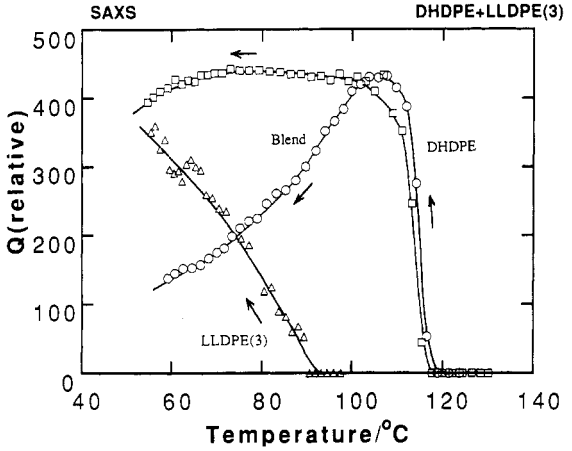

Figure 10. Temperature dependence of the invariance Q estimated using the SAXS data for the DHDPE + LLDPE(3) system.

scattering patterns when compared with those of the LLDPE(3) sample; the patterns of the blend can be assumed to consist mainly of the intense DHDPE scattering pattern with a small contribution of a weak and broad scattering from the LLDPE(3) component. The invariance Q is plotted against temperature in Figure 10, which is consistent with the WAXS data of Figure 9: the Q of the blend can be assumed as an overlap between those of the pure polymer of DHDPE and of LLDPE(3). In Figure 11 are plotted the interlamellar spacings against temperature for the three kinds of samples. It should be noted here that the long spacing is different from the simple average between that of the original DHDPE and of the LLDPE(3) polymer. The longer spacing exhibited by the blend indicates some coordinated spatial arrangement of DHDPE and LLDPE(3) lamellae which are separated from one another by a large amount of the amorphous phase including many branchings. The details will be discussed below.

(C) Structure of Blends. (i) DHDPE + LLDPE(2). As discussed in sections A and B, the blend of DHDPE with LLDPE(2) shows the cocrystallization phenomenon within the same lamella. It can be confirmed further by comparing the WAXS pattern before and after blending as shown in Figure 12. The position of the 110 reflection of the blend is close to that of LLDPE(2), but the 200 reflection is located at the 2θ position a little different

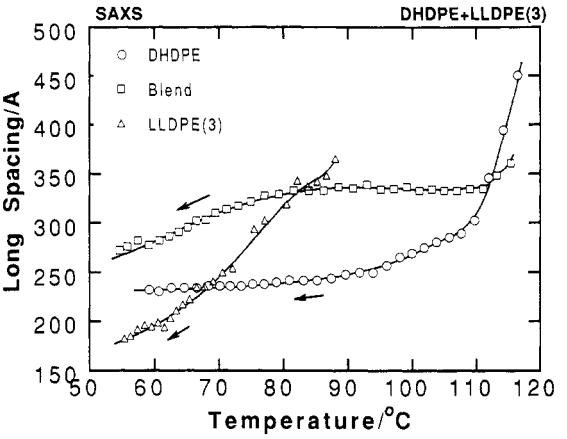

Figure 11. Temperature dependence of the long spacing estimated using the SAXS data for the DHDPE + LLDPE(3) system.

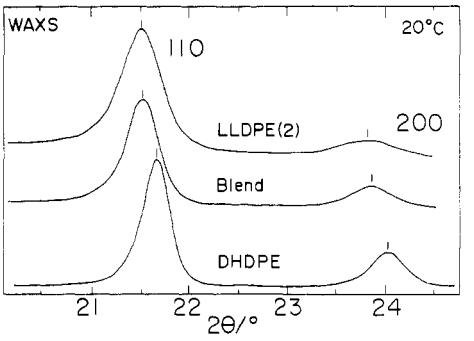

Figure 12. Comparison in the WAXS data measured at room temperature for the DHDPE + LLDPE(2) system.

Table II
Structural Data of PE Blends (Room Temperature)

	(WAXS) crystal cell, Å		(WAXS) crystallite size, Å		(SAXS)[a] long spacing, Å	(SALS) spherulite radius, μm
	a	b	[110]	[200]		
DHDPE	7.42	4.93	272	216	231	5.3
LLDPE(2)	7.48	4.96	184	134	158	9.3
blend	7.46	4.96	225	176	187	8.6
LLDPE(3)	7.63	5.03	117	100	195	2.4
blend	7.45[b]	4.96[b]	218[b]	190[b]	277	8.7

[a] At 60 °C. [b] Apparent [due to the overlapping of peaks of DHDPE and LLDPE(3)].

from those of the original ones. Table II lists the unit cell parameters a and b at room temperature: the cell parameters are closer to but a little smaller than those of LLDPE(2) because of the effect of coexisting DHDPE species. The effect of cocrystallization appears also in the crystallite size estimated from the half-width of the WAXS reflection and in the long spacing calculated from the SAXS pattern. It should be noted here that the peak positions of the first- and second-order scatterings of the SAXS pattern are also different between the three samples as shown in Figure 13. In Figure 14 the SALS pattern (H_V) is compared before and after blending of the DHDPE + LLDPE(2) system. Figure 15 shows the scattering profile measured along the 45° line of Figure 14 using an optical multichannel detector system. The estimated radius of the spherulite is between those of the original pure samples as listed in Table II.

By taking into account all these data of WAXS, SAXS, and SALS, the following structural view may be given for the DHDPE + LLDPE(2) blend system. The CD_2 and CH_2 stems are included in the same lamella and form the

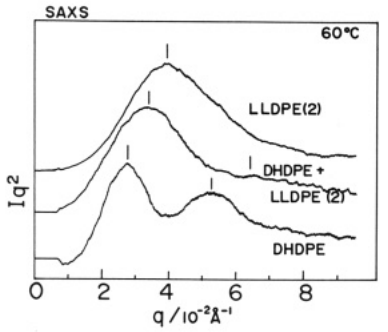

Figure 13. Comparison in the SAXS pattern measured at 60 °C for the DHDPE + LLDPE(2) system.

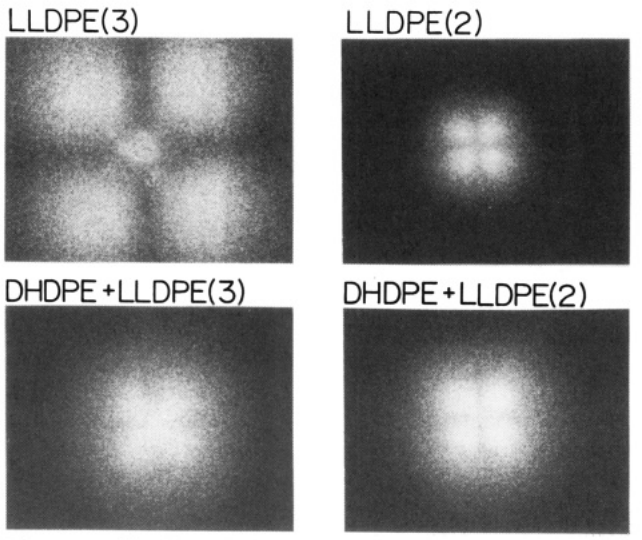

Figure 14. Small-angle light scattering patterns (H_V) measured at room temperature for the DHDPE blend systems with LLDPE-(2) and LLDPE(3) before and after blending.

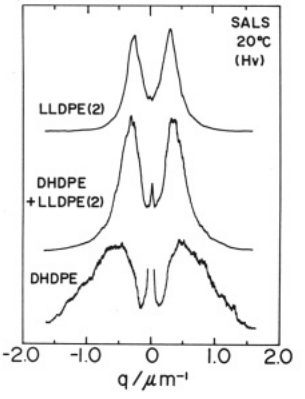

Figure 15. Comparison in the SALS pattern (H_V) measured at room temperature for the DHDPE + LLDPE(2) system.

cocrystals. The coexistence of the D and H species induces a change in the unit cell size, the crystallite size, and the interlamellar spacing (Table II). Furthermore, the spherulite radius is also modified by the cocrystallization effect. The coexistence of the D and H species is also related with the smaller Davydov splitting of the infrared crystalline bands[16] as seen in Figure 16. The relative position of the D and H stems in the crystallites should be clarified by calculating the distribution function which will be derived on the basis of the wide-angle and small-angle neutron scattering measurements, for example.

(ii) DHDPE + LLDPE(3). The blend of DHDPE and LLDPE(3) polymers shows some extent of a phase segregation between the two components. The WAXS patterns of the three samples measured at room temperature are compared in Figure 17. The X-ray reflections of the pure LLDPE(3) sample are broad and very weak when compared with those of DHDPE. The 110 reflection of the blend is asymmetric and can be assumed as an overlap between the intense DHDPE pattern and the weak and broad LLDPE(3) pattern, although the exact cell parameters in the blend are difficult to estimate. The infrared spectral data, however, indicate a more complicated situation than that speculated from the WAXS data. As seen in Figure 18, the CH_2 and CD_2 infrared bands show a different splitting width from those of the original pure components even though the phase separation occurs

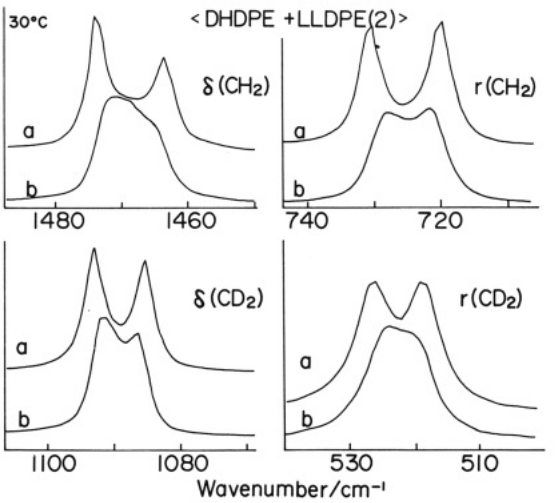

Figure 16. Comparison in the infrared spectral pattern at room temperature measured for the DHDPE + LLDPE(2) system: (a) pure LLDPE(2) or DHDPE; (b) the blend.

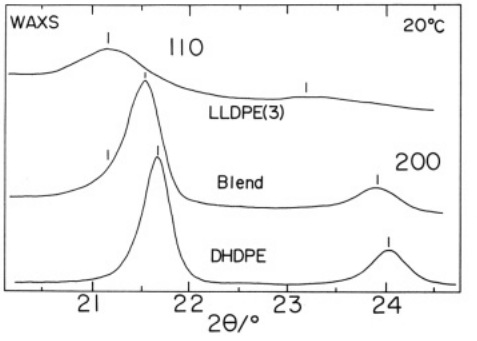

Figure 17. Comparison in the WAXS data measured at room temperature for the DHDPE + LLDPE(3) system.

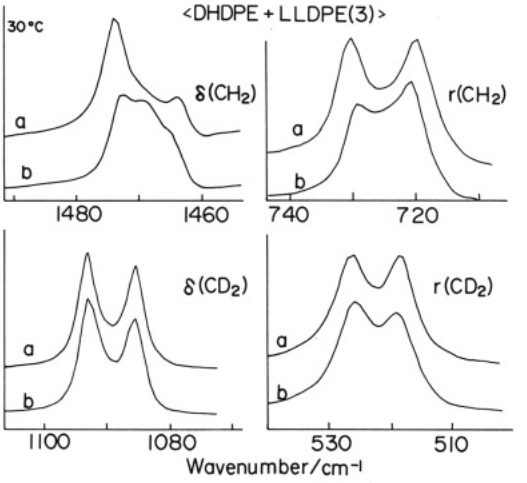

Figure 18. Comparison in the infrared spectral pattern at room temperature measured for the DHDPE + LLDPE(3) system: (a) pure LLDPE(3) or DHDPE; (b) the blend.

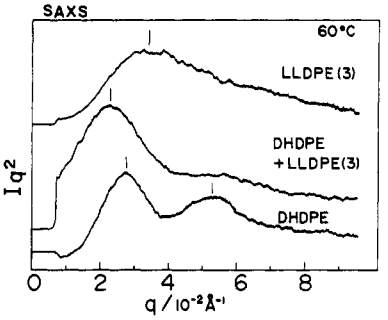

Figure 19. Comparison in the SAXS pattern measured at 60 °C for the DHDPE + LLDPE(3) system.

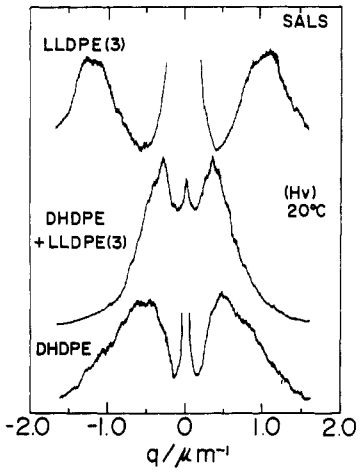

Figure 20. Comparison in the SALS pattern (H_V) measured at room temperature for the DHDPE + LLDPE(3) system.

to some extent. That is to say, the CH_2 and CD_2 chains are considered to interact to some extent by intrusion through the neighboring lamellae of the other species. Such an idea is consistent with the change in the SAXS pattern before and after blending. As seen in Figure 19, the peak position and pattern of the SAXS are very different in the blend than those of the pure components. The interlamellar spacing is longer than those of DHDPE and LLDPE-(3) samples prepared under almost the same conditions. In Figure 14 the SALS pattern of the blend is found quite different from that of the pure LLDPE(3) sample. Figure 20 clarifies this situation more clearly: the spherulite radius is increased by a factor of about 4 when compared with the original one (Table II). Therefore, the D and H lamellae are considered to be mixed together in the *same* spherulite and affected by each other through some side-by-side interactions. Such a situation can be detected also for the other blend systems utilized in the preceding paper:[13] DHDPE + HDPE, DHDPE + LLDPE(1), and DHDPE + LDPE, where the characterization of HDPE, LLDPE(1), and LDPE is referred to in the preceding paper. From these data we may say that the sample which shows the smaller spherulite size before blending can get the larger spherulite radius after blending (see the case of LLDPE(3)).

In Figure 21 are illustrated some possibilities of the aggregation structure of the D and H species in the blend sample. In these figures the white and black blocks indicate the lamellae of the H and D species, respectively. Model A where the H and D lamellae are stacked together in the same spherulite, is considered to be the case of DHDPE + LLDPE(3) blend system discussed above. The DHDPE + LLDPE(2) system is considered to fit the model D where the H and D species coexist in the same lamella as indicated by a checkered pattern of white and black

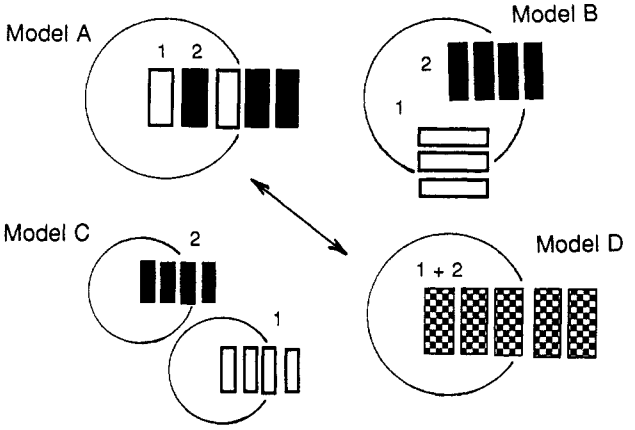

Figure 21. Aggregation models of the CH_2/CD_2 lamellae within the spherulites (refered to in the text). In these models the white and black blocks represent the H and D lamellae, respectively. The checkered pattern in model D illustrates a cocrystallized state of the H and D stems in the lamella.

blocks. Model B shows a coexistence of the axially-arrayed lamellar series consisting of only one species in the same spherulite. Model C is a coexistence of two types of spherulites in the sample, each of which consists of H or D species. The experimental data mentioned above cannot support the models B and C. We may conclude that the molecular chains in the present blend system may be aggregated in a form of structure located somewhere between models A and D: the DHDPE + LLDPE(2) is the closest to model D and the DHDPE + LLDPE(3) system has a structure closer to that of model A. The DHDPE + HDPE system may also have a similar structure to model A. Models A and D can be assumed to locate on a single line of structure and the transformation between models A and D is considered to be continuous, i.e., the degree of invasion of the CH_2 chain segments into the CD_2 lamellae (or vice versa) may continuously change between models A and D, depending on the degree of branching of the CH_2 species.

Concluding Remarks

In this paper the cocrystallization and phase segregation phenomena of the PE blend system consisting of D and H species have been confirmed by means of WAXS, SAXS, and SALS. The structure of the blend viewed from the characteristic length of dimension ranging from angstrom to micrometer has been discussed, and plausible models have been proposed. In addition to the WAXS, SAXS, and SALS data, the neutron scattering data, including both the small-angle and wide-angle scatterings, will help us to clarify the detailed spatial arrangements of the CD_2 and CH_2 chains in the lamellae and in the spherulites.

We may now have a question why such structures of a blend system as proposed above (Figure 21) should be obtained through the crystallization phenomenon during cooling from the melt. An investigation of the aggregation state of the D and H species in the melt may give us some indication for such a question.[17-23] Quantitative discussion on the interaction parameters between the D and H species may also give us useful information.[23] An investigation of nucleation and growth behaviors of crystalline lamellae during the crystallization process will be also required. All these problems are now being challenged.

Acknowledgment. We are grateful to the Exxon Chemicals Co., Ltd., for their kind supply and characterization of the PE samples. Support of this work by the

Department of Energy including the use of the SUNY X3A2 Beamline at the National Synchrotron Light Source is gratefully acknowledged.

References and Notes

(1) Norton, D. R.; Keller, A. *J. Mater. Sci.* **1984**, *19*, 447.
(2) Hu, S.; Kyu, T.; Stein, R. S. *J. Polym. Sci., Part B: Polym. Phys.* **1987**, *25*, 71.
(3) Kyu, T.; Hu, S.; Stein, R. S. *J. Polym. Sci., Part B: Polym. Phys.* **1987**, *25*, 89.
(4) Ree, M.; Kyu, T.; Stein, R. S. *J. Polym. Sci., Part B: Polym. Phys.* **1987**, *25*, 105.
(5) Vadhar, P.; Kyu, T. *Polym. Eng. Sci.* **1987**, *27*, 202.
(6) Marand, H. L.; Stein, R. S.; Stack, G. M. *J. Polym. Sci., Part B: Polym. Phys.* **1988**, *26*, 1361.
(7) Rego Lopez, J. M.; Gedde, U. W. *Polymer* **1988**, *29*, 1037.
(8) Rego Lopez, J. M.; Conde Brana, M. T.; Terselius, B.; Gedde, U. W. *Polymer* **1988**, *29*, 1045.
(9) Rego Lopez, J. M.; Gedde, U. W. *Polymer* **1989**, *30*, 22.
(10) Hosoda, S.; Gotoh, Y. *Polym. J.* **1988**, *20*, 17.
(11) Song, H. H.; Stein, R. S.; Wu, D. Q.; Ree, M.; Philips, J. C.; Legrand, A.; Chu, B. *Macromolecules* **1988**, *21*, 1180.
(12) Song, H. H.; Wu, D. Q.; Chu, B.; Satkowski, M.; Ree, M.; Stein, R. S.; Philips, J. C. *Macromolecules* **1990**, *23*, 2380.
(13) Tashiro, K.; Stein, R. S.; Hsu, S. L. *Macromolecules*, preceding paper in this issue.
(14) Strobl, G. R.; Schneider, M. J. *J. Polym. Sci.: Polym. Phys. Ed.* **1980**, *18*, 1343.
(15) Strobl, G. R.; Schneider, M. J.; Voigt-Martin, I. G. *J. Polym. Sci.: Polym. Phys. Ed.* **1980**, *18*, 1361.
(16) Cheam, T. C.; Krimm, S. *J. Polym. Sci.: Polym. Phys. Ed.* **1981**, *19*, 423.
(17) Stehling, F. C.; Ergos, E.; Mandelkern, L. *Macromolecules* **1971**, *4*, 672.
(18) Schelten, J.; Wignall, G. D.; Ballard, D. G. H.; Longman, G. W. *Polymer* **1977**, *18*, 1111.
(19) Stamm, M.; Fischer, E. W.; Dettenmaier, M.; Convert, P. *Faraday Discuss. Chem. Soc.* **1979**, *68*, 263.
(20) Schelten, J.; Ballard, D. G. H.; Wignall, G. D.; Longman, G.; Schmatz, W. *Polymer* **1976**, *17*, 751.
(21) Nicholson, J. M.; Finerman, T. M.; Crist, B. *Polymer* **1990**, *31*, 2287.
(22) Wignall, C. D.; Bates, F. S. *Makromol. Chem., Macromol. Symp.* **1988**, *15*, 105.
(23) Rhee, J.; Crist, B. *Macromolecules* **1991**, *24*, 5663.